ELSEVIER

Coordination Chemistry Reviews
208 (2000) 33–45

COORDINATION
CHEMISTRY
REVIEWS

www.elsevier.com/locate/ccr

Photoinduced multielectron charge transfer processes in Group 8 — platinum cyanobridged supramolecular complexes

Clark C. Chang, Brian Pfennig, Andrew B. Bocarsly *

Department of Chemistry, Frick Laboratory, Princeton University, Princeton, NJ 08544-1009, USA

Received 9 July 1999; accepted 4 November 1999

Contents

Abstract

Mixed valence compounds have attracted considerable attention because of their capability for photoinduced electron transfer, which has potential applications in energy conversion and photocatalysis. In such applications, the ability to transfer multiple electrons with a single photon is desirable. Symmetric, multinuclear complexes of the form $[L(NC)_4M(II)–CN–Pt(IV)(NH_3)_4–NC–M(II)(CN)_4L]^{4-}$ (where M is a Group 8 metal and L is a CN^- or a σ-donor ligand) provide for such photoinduced multielectron charge transfer processes. These complexes exhibit intense metal–metal charge transfer (MMCT) bands in

---

* Corresponding author. Tel.: + 1-609-2583888; fax: + 1-609-2582383.
E-mail address: bocarsly@chemvax.princeton.edu (A.B. Bocarsly).

PII: S0010-8545(99)00245-3

the blue portion of the spectrum (350–450 nm). In the case where M = Fe, irradiation into the MMCT band centered at 425 nm produces a net two electron charge transfer with a quantum yield of 0.01. The observed reaction is found to yield only two electron products. Well defined oligomers and polymers of the iron based system can be synthesized either as soluble materials or adherent films on electrode surfaces. The photochemical reactivity and photophysics of these species are found to be a function of molecular geometry. In the case of the polymeric systems, one-dimensional, two-dimensional, and network materials can be synthesized, using electrochemical techniques, to control the polymer reactivity sites. Polymer modified electrodes exhibit a photocurrent response which is diagnostic for the photochemistry occurring within the film. The redox potential of the primary photoproducts are found to be very sensitive to the number of bridging cyanide ligands per iron center and thus, to the degree of branching of the polymer. Correctly selected polymer morphologies lead to primary photoproducts on the electrode surface which are capable of oxidizing chloride to chlorine. This chemistry can be used to produce a photochemical energy conversion cycle in which visible light induces the oxidation of halides to energy rich halogens.

Keywords: Photochemistry; Coordination; Polymer; Halide; Oxidation

1. Introduction

Mixed valence complexes are capable of transferring an electron from one localized state to another upon absorption of a photon [1,2]. This phenomenon, termed photoinduced electron transfer, has led to the investigation of mixed valence compounds for their potential applications in the conversion of optical energy to chemical energy. This separation of charge is usually evidenced by a change in the oxidation state of the donor and acceptor metal centers in the complex, which can be used in a variety of practical applications like photocatalysis, organic synthesis, reduction of carbon dioxide or water splitting [3–6]. These applications are often multielectron transformations, and the energy input required to perform these reactions are inversely related to the number of electrons transferred in the catalytic step [7]. Pathways involving multiple electron oxidations are thus thermodynamically favored over pathways involving only one electron. Several systems have been developed which are capable of providing multiple electrons, for example, linking several chromophores onto a polymer backbone allows the accumulation of multiple redox equivalents through the absorption of multiple photons (one photon/electron at each chromophore) [8–10]. Similarly, polynuclear complexes in which several donors are linked to a single unit can also be used to absorb multiple photons and store charge [11–13]. In all these systems, only one electron is transferred per photon absorbed; a fundamentally different approach would be to transfer multiple electrons with a single photon, so-called photoinduced multielectron charge transfer [14].

Platinum seems to be suited ideally as the basis for a complex capable of carrying out photoinduced multielectron charge transfer because of the stability of Pt(II) and

Pt(IV) complexes and the short-lived and unstable nature of Pt(III). Furthermore, because of the preference of Pt(II) for a square planar geometry and Pt(IV) for an octahedral structure, charge transfer can also induce the formation and breaking of coordinate covalent bonds. Thus, coupling a Pt(IV) unit as an electron reservoir with two 1e$^-$ donors could lead to a 2e$^-$ transfer process. Assuming a stepwise electron transfer mechanism, photoexcitation of the Pt-based molecule will cause a single electron to hop from one of the electron donors to the Pt center, generating the unstable Pt(III) state. From this intermediate, two rapid thermal reactions are possible; back electron transfer to regenerate the initial Pt(IV) complex with no net chemistry, or electron transfer from the other donor to create Pt(II), an oxidation state that differs by two electrons from the reactant. Thus, it is possible to design species that would be capable of two-electron charge transfer upon excitation with a single photon.

2. Synthesis of two-electron charge transfer species

Following the above strategy, we have reported on the syntheses of a series of trinuclear complexes of the form $[\mathrm{L(NC)_4M(II)–CN–Pt(IV)(NH_3)_4–NC–M(II)(CN)_4L}]^{4-}$, where M = Fe, Ru, or Os, and L = CN$^-$ or a σ-donor ligand [15–17]. The parent complex which has M = Fe and L = CN$^-$ will be identified as 3-HCFPA (a hexacyanoferro platinum amine molecule with three metal centers). These compounds were found to exhibit an intense absorption in the visible portion of the spectral region. Because the energy of the absorption was found to vary with the redox potential of the $\mathrm{M(CN)_5L}$ moiety brought about by variation of M and L, this absorption feature was assigned as a metal–metal charge transfer (MMCT) band [15,16]. These complexes were synthesized by a redox reaction between $[\mathrm{M(III)(CN)_5L}]^{3-}$ and $[\mathrm{Pt(II)(NH_3)_4}]^{2+}$ in aqueous solution, and it was found that irradiation into the MMCT of the trinuclear complex produced a net two electron charge transfer which dissociates the complex into its starting reagents, as shown in Eq. (1) for 3-HCFPA [15].

$$[\mathrm{(NC)_5Fe(II)-CN-Pt(IV)(NH_3)_4-NC-Fe(II)(CN)_5}]^{4-} \xrightarrow{h\nu} 2[\mathrm{Fe(III)(CN)_6}]^{3-} + [\mathrm{Pt(II)(NH_3)_4}]^{2+} \qquad (1)$$

Since the dissociation products are the starting reagents, the original trinuclear complex can be regenerated if the reaction mixture is kept in the dark (the reverse of Eq. (1)).

While 3-HCFPA is an intriguing complex for studying 2e$^-$ charge transfer, ultimate application of it for the collection, storage and reclamation of optical energy will be in the form of larger supramolecular species like oligomers and polymers. Since the trinuclear species is synthesized by a redox reaction in which the $[\mathrm{Fe(III)(CN)_6}]^{3-}$ moiety is reduced to $[\mathrm{Fe(II)(CN)_6}]^{4-}$ upon complexation with Pt(II), it was proposed that the iron center could be reoxidized to Fe(III) which would restore its reactivity towards Pt(II) [18]. Thus, if the irons in the trinuclear species were reoxidized, it should be possible to link together two trinuclear species through a bridging Pt to form a seven metal species, as illustrated in Fig. 1. Since the irons at either end of the chain remain in the oxidized state, these irons can also react with Pt(II) to form longer species. It should be noted that the irons in the middle of the oligomer chain are in the reduced state and are incapable of reaction with Pt. Thus, polymer growth can only occur at the ends of the chain, such that all the oligomers formed in this synthesis are one-dimensional chains [18]. Since this oligomerization is carried out by simply mixing oxidized 3-HCFPA with Pt(II) salt, there are a large number of chain lengths possible. This distribution of chain lengths can be weighted towards longer chain lengths by using a higher molar fraction of Pt; the mixture of chain lengths has been successfully separated using size exclusion chromatography. The oligomer fractions can be characterized using an end-group analysis. Since irons with one bridging cyanide (terminal irons) have a redox potential of $E_{1/2} = +0.54$ V versus SCE, and irons with two bridging cyanides (interior irons) have a redox potential of $E_{1/2} = +0.85$ V versus SCE, it is possible to determine the relative concentrations of singly and doubly bridged iron species through an electrochemical technique like cyclic voltammetry [18]. A higher relative concentration of doubly bridged iron species would indicate a longer chain length.

It can be seen that the iron centers in an oligomer act as a switch to determine whether chain extension can occur at that position. Because the interior irons in the linear chain oligomers remained in the 2+ oxidation state, chain extension could

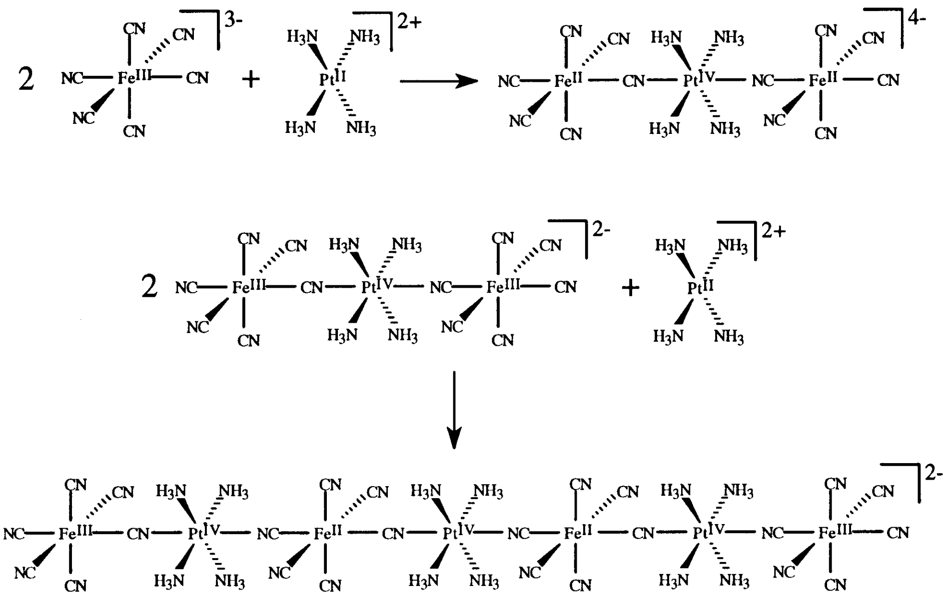

Fig. 1. Synthetic reactions for formation of the trinuclear species and heptanuclear species.

not occur at those sites. However, if they were to be oxidized and thus restore their reactivity, chain growth can occur in the middle of an oligomer chain to form branched species [18]. This can be done electrochemically by holding a working electrode at a potential above the redox potential of the doubly bridged iron center while immersed in a solution of 3-HCFPA and excess $[Pt(NH_3)_4]^{2+}$. A branched polymer (dubbed poly-HCFPA) [18–21] based on 3-HCFPA as a monomeric unit forms which is insoluble and precipitates onto the working electrode as a thin layer. The coordination polymer thickness and degree of crosslinking are characterized by visible light interferometry and cyclic voltammetry [18]. Because the redox potential of the iron center is dependent on the number of cyanides which are bridged to Pt (roughly +300 mV for each additional bridging cyanide), cyclic voltammetry can be used to determine the relative concentration of irons with different numbers of bridging cyanides [18,20]. The extent of polymer crosslinking is expressed as the average number of bridging cyanides per iron center; if this value is close to 2, then the polymer structure is predominantly one-dimensional, while a higher value would indicate a two or three-dimensional network. Both the thickness and the degree of crosslinking are easily controlled by variation of the synthetic conditions. It was found that although both time as well as the potential of polymerization had an effect on polymer characteristics, the thickness of the film was primarily controlled by the time of polymerization while the degree of crosslinking could be increased by raising the potential of polymerization [18]. With such a high degree of control over polymer film characteristics, it was possible to synthesize a polymer film with the desired characteristics; for example, a series of films with the same thickness but with increasing crosslinking could be easily generated.

3. Photochemistry of coordination oligomers and polymers

3.1. Design of photoelectrochemical experiments

Previously, the photochemical reactivity of thin polymer films allowed the films to be used in photolithography to build high spatial resolution structures composed of different polynuclear hexacyanometalates [21]. These electrochromic materials have potential application as light-modulating devices; a two-color diffraction grating has been synthesized which can be controlled dynamically based on the applied electrode potential [20]. While the appearance of the photodissociation products for 3-HCFPA has been demonstrated using UV–vis spectroscopy, poly-HCFPA photochemistry has been difficult to characterize similarly due to the insolubility of the polymer and the complexity of the system. Therefore, two photoelectrochemical experiments were devised to determine the identity of the photoproducts as well as the quantum yield [22]. One experiment characterizes the photoproducts on the basis of the $E_{1/2}$ by observing the dependence of the photocurrent on the working electrode potential. There is a cathodic photocurrent for a species being reduced if the electrode is at a potential below the redox potential of the photogenerated species, and this cathodic photocurrent is expected to decrease as the applied potential is raised above E^0_R of the photoproduct. For example, the expected photoproduct from photolysis of 3-HCFPA is ferricyanide, which has an $E^0_R = +0.2$ V versus SCE. At potentials less than +0.2 V versus SCE, there is expected to be a cathodic photocurrent from the reduction of ferricyanide, while at potentials above +0.2 V versus SCE, no photocurrent is anticipated. This experiment can be accomplished by slowly ramping the applied potential while the electrode is irradiated. Because of variation in the dark current as the potential is increased due to electrochemistry of other species in solution, the light is chopped to distinguish between the dark background current and the current from the reduction of the photogenerated species. This technique will be referred to as linear sweep photovoltammetry (LSPV). The second experiment is coulometric in nature and involves holding the working electrode at a potential below E^0_R for all photoproducts. Integration of the cathodic photocurrent then allows determination of the quantum yield for photolysis based on the number of electrons collected at the electrode.

3.2. Verification of photoelectrochemical techniques

As reported in Eq. (1), photolysis of 3-HCFPA leads to the formation of ferricyanide and $[Pt(NH_3)_4]^{2+}$. The latter product is not electroactive for kinetic reasons, however, photo-generated ferricyanide can be detected via generation of a current at an electrode poised negative of the ferro/ferricyanide redox potential. The photogeneration of ferricyanide is confirmed by analysis of a solution of 3-HCFPA in 0.1 M $NaNO_3$ using LSPV by scanning an ITO electrode from 0 to 0.4 V versus SCE with a sweep rate of 0.5 mV s^{-1}. Illumination from an Ar^+ laser (488 nm) was chopped at 25 mHz (112 mW cm^{-2} incident intensity) resulting in the trace shown in Fig. 2a. The inset of Fig. 2a shows the magnitude of the photocurrent ($i_{h\nu} - i_{dark}$) versus applied potential. The sigmoidal relationship is similar to that obtained using classic steady-state voltammetry. This indicates that the photoproduct has an $E_{1/2}$ of +0.2 V versus SCE consistent with the $[Fe(II/III)(CN)_6]^{4-/3-}$ redox potential, and consistent with previously reported spectroscopic evidence. Thus, these data suggest the reaction scheme presented in Eq. (2) [22].

$$\begin{aligned}&[Fe(II)(CN)_6 - Pt(IV)(NH_3)_4 - Fe(II)(CN)_6]^{4-} \xrightarrow{h\nu} 2Fe(CN)_6^{3-}\\&\quad + Pt(NH_3)_4^{2+} \text{ (in solution)}\\&2f_{col}Fe(CN)_6^{3-} \xrightarrow{2e^-} 2f_{col}Fe(CN)_6^{4-} \text{ (at electrode surface)} \qquad (2)\end{aligned}$$

where f_{col} is the collection efficiency, representing the number of electrons collected at the electrode from ferricyanide reduction compared to the total amount of ferricyanide generated from photolysis.

For the purposes of determining quantum yield, it is interesting to examine the current–time behavior from illumination of a cell containing 3-HCFPA. Fig. 2b shows a series of photocurrent transients from illumination of a solution of 3-HCFPA at various intensities (488 nm). Since the identified product (ferricyanide) is electrochemically quasireversible [23], the current observed is controlled by the

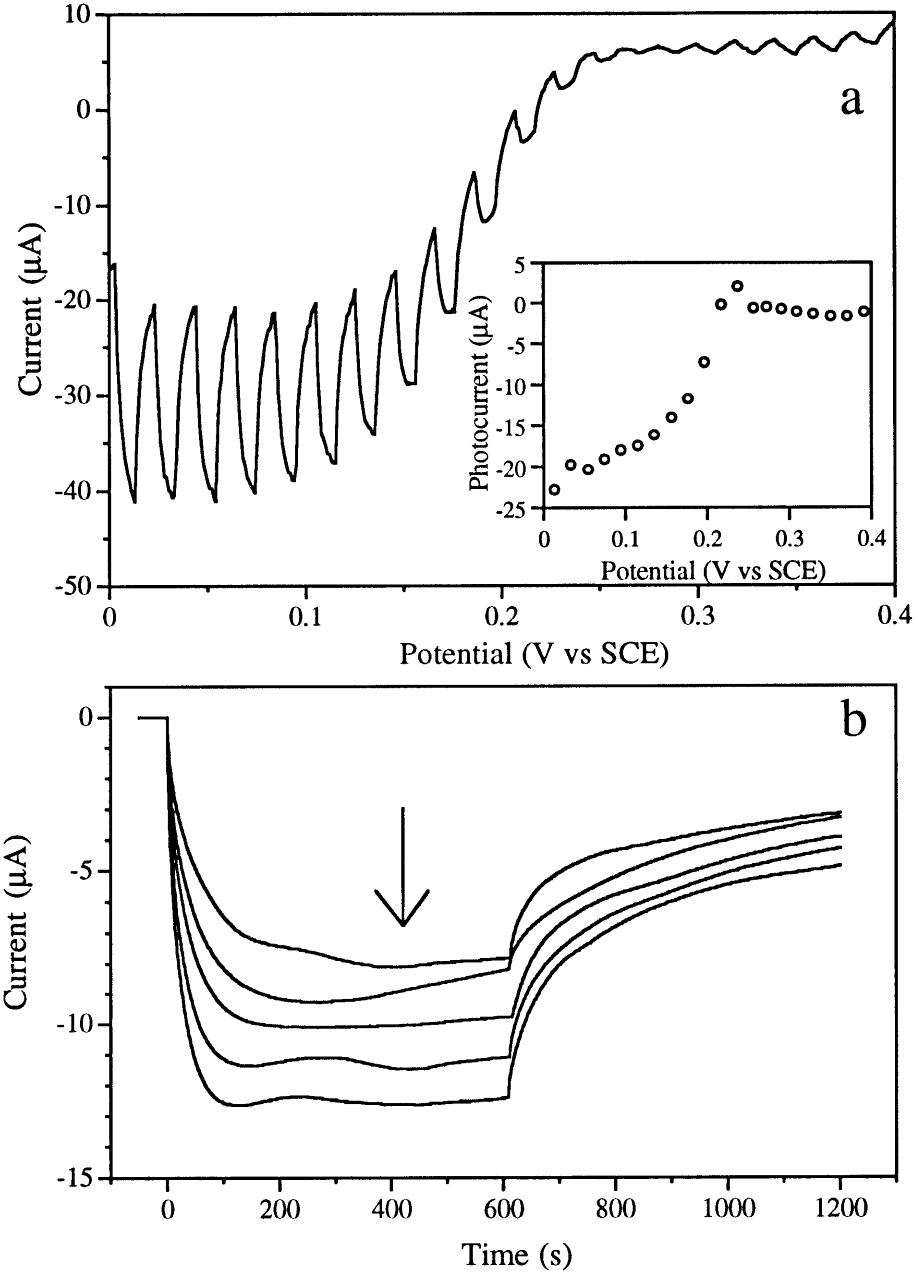

Fig. 2. (a) Linear sweep photovoltammetry (technique described in text) of 2.5 mM 3-HCFPA in 0.1 M $NaNO_3$. Inset shows peak photocurrent in each pulse versus potential, with the characteristic shape of a steady-state voltammogram with $E_{1/2} = +0.2$ V versus SCE; (b) Photocurrent transients of a solution of 0.34 mM 3-HCFPA in 0.1 M $NaNO_3$ illuminated at various intensities. Irradiation in each experiment began at $t = 0$ s, and stopped at $t = 600$ s. Arrow indicates increasing light intensity.

concentration of this species in solution as well as the rate at which the charge is transferred to the electrode by diffusion. Additionally, there is a decrease in the rate of the ferricyanide generation during the course of the experiment as the optical density (Fig. 2a, inset) of the solution decreases with disappearance of 3-HCFPA. The roughly steady-state value the photocurrent reaches can be understood as the point where the rate of the ferricyanide generation from photodissociation is balanced by the rate of the ferricyanide reduction through diffusion to the electrode surface. This steady-state value increases with increasing intensity since the concentration of ferricyanide is increased. When the light is turned off, the current decays with a $t^{-1/2}$ dependence, consistent with a diffusion controlled reduction of ferricyanide.

A quantum yield of $\Phi_{\mathrm{dis}} = 0.01$ is calculated for the disappearance of 3-HCFPA by UV–vis spectroscopy. Since two ferricyanide units are generated for each 3-HCFPA photodissociated, the quantum yield for ferricyanide generation is 0.02. The quantum yield for electron flow is $\Phi_{\mathrm{e}} = 1.4 \times 10^{-3}$. Thus the collection efficiency is $f_{\mathrm{col}} = 0.07$, that is, 7% of the photochemically generated ferricyanide is reduced at the electrode. This value is found to be independent of light intensity as well as concentration of 3-HCFPA in the cell, however, because of the dependence of Φ_{e} on photoproduct diffusion, f_{col} is expected to vary if the geometry of the photoelectrochemical cell is changed.

4. Photochemistry of the coordination polymer

The photovoltammetric response of surface confined poly-HCFPA is shown in Fig. 3. In contrast to 3-HCFPA, this experiment shows that a cathodic photocurrent is generated at potentials positive of the $E_{1/2}$ of ferricyanide. Also, the charge collected during photolysis is greater than the amount of ferricyanide observed in solution using UV–vis spectroscopy. These results preclude dissolved ferricyanide as the only photoproduct. As evidenced by cyclic voltammetry of the polymer films, there exist a distribution of irons with different number of bridging cyanides within the polymer film. For irons having multiple bridging cyanides, it is difficult to envision a single photon process which would produce free ferricyanide. Rather, we would expect that one photon is required to break each bridge. Since the iron center is oxidized during bond breakage, then it can be reduced multiple times, thus the observation of more than one electron injected per ferricyanide generated in solution. This leads to the proposed mechanism shown in Fig. 4. Consider an iron center that has formed three bridges (shown at the top of Fig. 4). Upon absorption of a photon, one of the bridges is broken by the photoinduced charge transfer, leaving the iron center in the oxidized state still with two bridges (step a). This iron center can then be reduced directly at the electrode with injection of an electron at + 0.85 V, the redox potential of a doubly bridged iron (step b). This iron center can undergo subsequent light absorption and photolysis. An oxidized iron center is generated each time a bridge is broken (step c) until there are no bridges left and free ferrocyanide is generated (step d). Thus, according to this mechanism, an iron

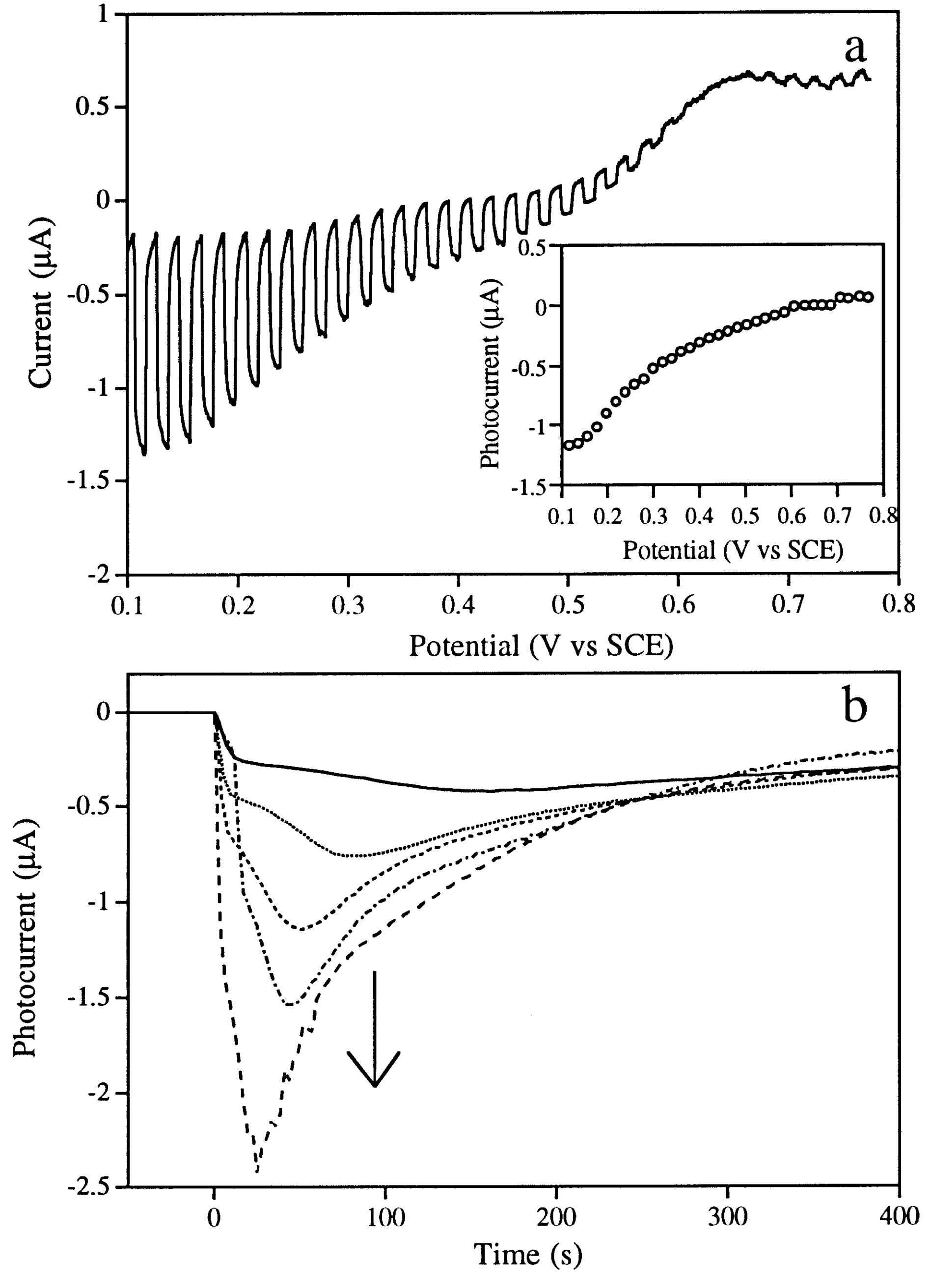

Fig. 3. (a) Linear sweep photovoltammetry of a polymer film (polymerized at 1 V for 1000 s) immersed in 0.1 M $NaNO_3$. Inset shows peak photocurrents in each pulse with a cathodic photocurrent present at potentials greater than the $[Fe(CN)_6]^{3-/4-}$ couple; (b) Photocurrent transients of a polymer film (polymerized at 1.2 V for 636 s) irradiated at various intensities. Arrow indicates increasing intensity.

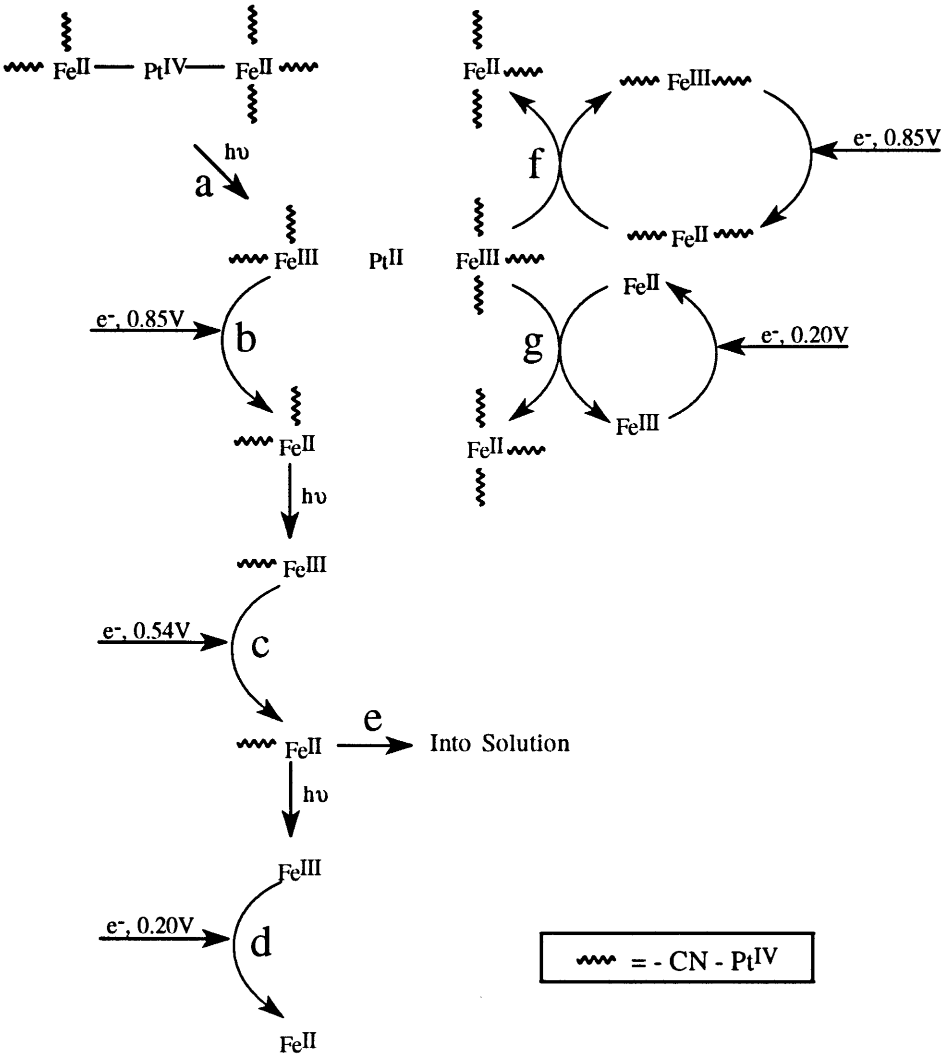

Fig. 4. Proposed mechanism for the photochemical decomposition of a polymer film which shows the possibility of multiple ferricyanide reduction steps to account for the observation of more electrons collected at the electrode relative to the amount of ferricyanide photogenerated.

center can be reduced as many times as there are cyano-platinum bridges to break. This can be verified by synthesizing a series of films in which the average number of bridging cyanides per iron center is varied. The collection efficiency for these films varied in a fashion directly proportional to the degree of branching of the polymer film. However, the number of bridging cyanides on an iron center is considered a theoretical maximum for the number of electrons collected since the iron center can be part of an oligomer fragment that is no longer tethered to the electrode surface and diffuses away (step e). Steps f and g illustrate mediated charge transfer to surrounding polymer fragments if charge transfer to the electrode surface is hindered.

Based on the model advanced, the photochemically generated ferricyanide centers should not only be capable of reduction by the electrode surface, but also be capable of reduction by solution species. An interesting feature of the photodissociation process in the polymer is the creation of strongly oxidizing ground state ferricyanide centers. Comparison of the relative redox potentials of iron centers with different numbers of bridged cyanides and the redox potential of the halides reveals the possibility of oxidizing the halides to the corresponding halogen (Fig. 5) [24]. As shown in Fig. 5, I^- can be oxidized by irons with at least one bridging cyanide. A highly networked polymer film (polymerized at + 1.4 V versus SCE for 500 s) was irradiated in the presence of 0.1 M NaI. A quantum yield of $\Phi_I = 6.1 \times 10^{-3}$ for generation of I_3^- was spectroscopically determined. Bromide oxidation ($E_R^0 = +0.85$ V versus SCE) [24] requires an iron center with at least two bridging cyanides ($E_{1/2} = +0.85$ V versus SCE), and so while we do expect bromide oxidation to take place, there are less irons available capable of oxidizing Br^- as compared to I^-. This observation easily explains the lower quantum yield for Br_2 production by irradiation of the same highly networked polymer film (polymerized at + 1.4 V versus SCE for 500 s), $\Phi_{Br} = 4.1 \times 10^{-3}$. This trend continues with the Cl^-/Cl_2 couple. Since this couple has the highest redox potential of the three halides studied ($E_R^0 = +1.12$ V versus SCE) [24], it is also the most selective since chloride can only be oxidized by iron centers with at least four bridging cyanides ($E_{1/2} = +1.27$ V versus SCE, Fig. 5). Thus, it has the smallest quantum yield,

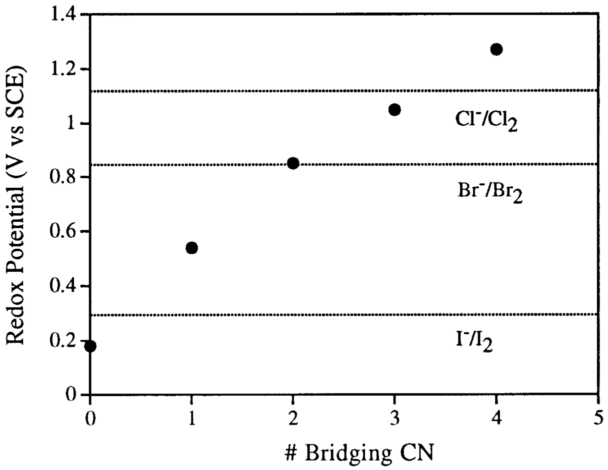

Fig. 5. Relative values of $E_{1/2}$ for irons with different numbers of bridging cyanides, and halide/halogen couples.

$\Phi_{Cl} = 8.7 \times 10^{-4}$ (as determined spectrophotometrically), for halide oxidation of the three halides tested. The dependence of halogen production on polymer morphology follows the anticipated pattern based on the model put forth. A lightly crosslinked film synthesized at $+0.9$ V versus SCE for 200 s which is composed primarily of iron centers with three bridging cyanides or less is incapable of carrying out the photo-oxidation of Cl^- to Cl_2, although the formation of Br_2 and I_2 was still observed.

5. Energy conversion

Of practical interest, is the finding that at open circuit, highly crosslinked poly-HCFPA allows for the photochemical conversion of Cl^- to Cl_2, a process which results in the net conversion of optical energy to chemical energy. An energy diagram for this conversion is shown in Fig. 6. The efficiency of this process (η) can be defined as the ratio of the chemical energy gained to the energy of light used to initiate the reaction, as shown in Eq. (3).

$$\eta = \frac{\text{chemical energy}}{\text{light energy}} \tag{3}$$

The net free energy change for the photolysis of poly-HCFPA and subsequent generation of Cl_2 can be calculated using the known redox potentials of the iron and platinum metal centers as well as the redox potential of Cl^-. Based on this value, we calculate an approximate conversion efficiency of 0.07%. However, it is clear that the oxidation of halides can be accomplished using visible photons ($\lambda < 500$ nm), and that applications may be possible in the area of solar energy conversion.

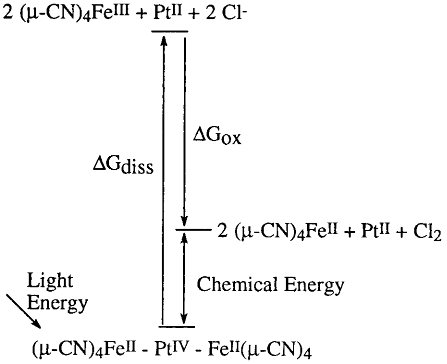

Fig. 6. The conversion of light energy to chemical energy using the photooxidation of Cl^- by highly bridged ferricyanide species within poly-HCFPA.

Acknowledgements

Support by the National Science Foundation is acknowledged under Grant no. CHE-9631380.

References

[1] K. Kalyanasundaram, M. Gratzel, in: R. Ugo, B.R. James (Eds.), Catalysis by Metal Complexes, Kluwer Academic, Boston, 1993.
[2] V. Balzani, A. Credi, M. Venturi, Coord. Chem. Rev. 171 (1998) 3.
[3] J.P. Collin, J.P. Sauvage, Coord. Chem. Rev. 93 (1989) 245.
[4] B.A. Gregg, M.A. Fox, A.J. Bard, Tetrahedron 45 (1989) 4707.
[5] T. Shiragami, C. Pac, S. Yanagida, J. Phys. Chem. 94 (1990) 504.
[6] G. Knor, Coord. Chem. Rev. 171 (1998) 61.
[7] J.A. Gilbert, D.S. Eggleston, W.R. Murphy, D.A. Geselowitz, S.W. Gersten, D.J. Hodgson, T.J. Meyer, J. Am. Chem. Soc. 107 (1985) 3855.
[8] J.N. Younathan, S.F. McClanahan, T.J. Meyer, Macromolecules 22 (1989) 1048.
[9] L.A. Worl, G.F. Strouse, J.N. Younathan, S.M. Baxter, T.J. Meyer, J. Am. Chem. Soc. 112 (1990) 7571.
[10] S.M. Baxter, W.E. Jones, E. Danielson, L. Worl, G. Strouse, J. Younathan, T.J. Meyer, Coord. Chem. Rev. 111 (1991) 47.
[11] A.A. Vlcek, Coord. Chem. Rev. 43 (1982) 39.
[12] D. Astruc, Comm. Inorg. Chem. 6 (1987) 61.
[13] M.J.S. Dewar, J.D. Dunitz, K. Hafner, S. Ito, J.-M. Lehn, K. Niedenzu, K.N. Raymond, C.W. Rees, F. Vogtle, Topics in Current Chemistry, Springer–Verlag, New York, 1990.
[14] B.W. Pfennig, A.B. Bocarsly, Comm. Inorg. Chem. 13 (1992) 261.
[15] M. Zhou, B.W. Pfennig, J. Steiger, D. Van Engen, A.B. Bocarsly, Inorg. Chem. 29 (1990) 2457.
[16] B.W. Pfennig, A.B. Bocarsly, J. Phys. Chem. 96 (1992) 226.
[17] Y. Wu, B.W. Pfennig, S.L. Sharp, D.R. Ludwig, C.J. Warren, E.P. Vicenzi, A.B. Bocarsly, Coord. Chem. Rev. 159 (1997) 245.
[18] C. Chang, D. Ludwig, A. Bocarsly, Inorg. Chem. 37 (1998) 5467.
[19] B.W. Pfennig, A.B. Bocarsly, Inorg. Chem. 30 (1991) 666.
[20] Y. Wu, B.W. Pfennig, E.P. Vicenzi, A.B. Bocarsly, Inorg. Chem. 34 (1995) 4262.
[21] A.B. Bocarsly, C.C. Chang, Y. Wu, E.P. Vicenzi, J. Chem. Ed. 74 (1997) 663.
[22] C.C. Chang, A.B. Bocarsly, J. Electroanal. Chem. 470 (1999) 99.
[23] D. Pletcher, C. Beriet, J. Electroanal. Chem. 361 (1993) 93.
[24] W.M. Latimer, Oxidation Potentials, Prentice-Hall, Englewood Cliffs, NJ, 1952.